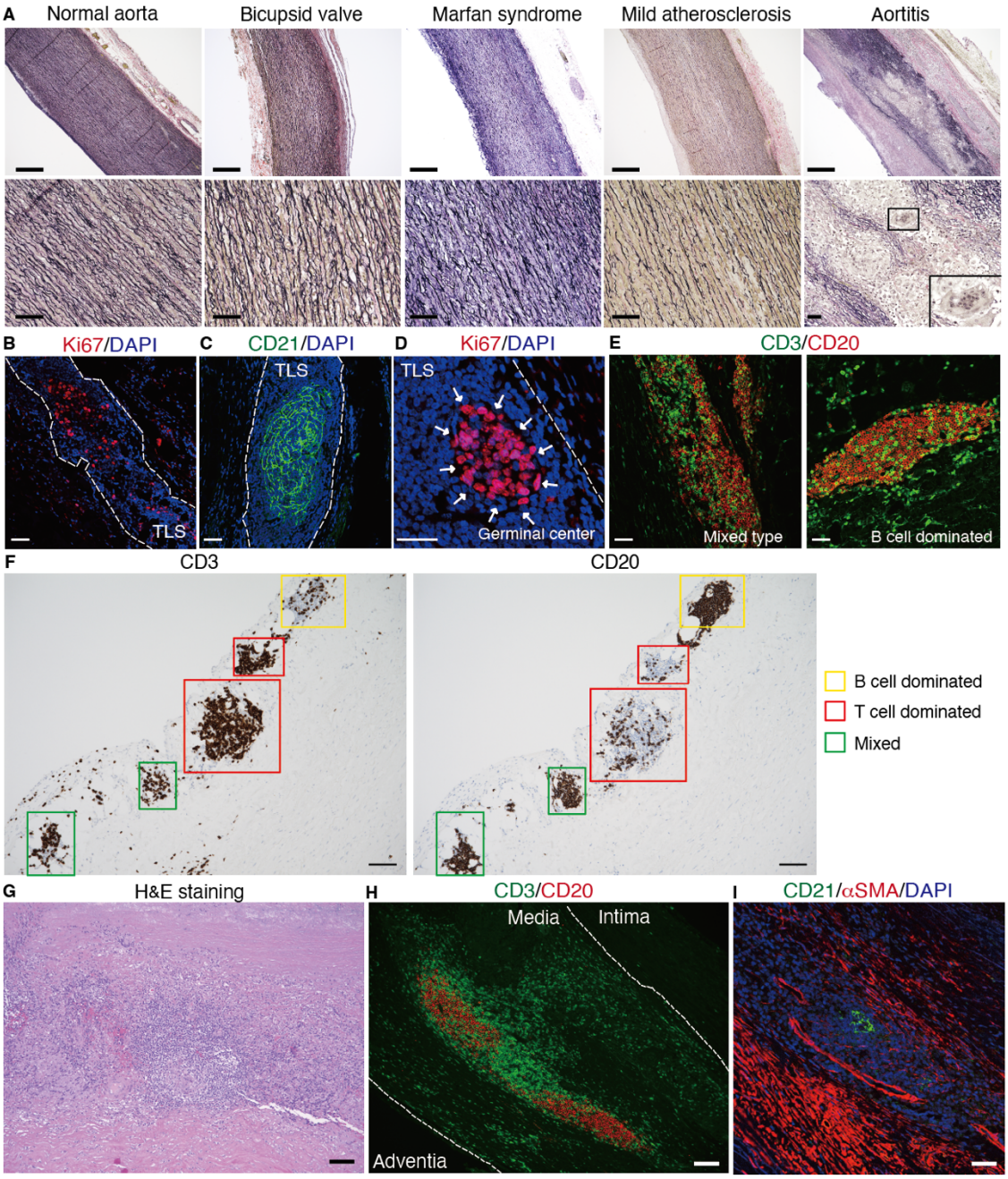
A
Normal aorta
Bicupsid valve
Marfan syndrome
Mild atherosclerosis
Aortitis
B
Ki67/DAPI
TLS
C
CD21/DAPI
TLS
D
Ki67/DAPI
TLS
Germinal center
E
CD3/CD20
Mixed type
B cell dominated
F
CD3
CD20
B cell dominated
T cell dominated
Mixed
G
H&E staining
H
CD3/CD20
Media
Intima
Adventia
I
CD21/αSMA/DAPI

fig. S1. Immunohistochemical analysis of ascending aortic aneurysms. (A) Histological analyses of different pathologies in the ascending aorta are displayed. Elastic tissue fibers are visualized by Verhoeff-Van Gieson (VVG) staining. Specimens from cases of autoimmune vasculitis show wall destruction, mononuclear cell infiltrates, and giant cell formation (insert). Scale bars, 500 μm (upper) and 50 μm (lower). **(B to I)** Immunohistochemical analysis of tertiary lymphoid structures (TLS) in the aortic adventitia **(B to F)** and the media **(G to I)** are shown. Immunofluorescence was used to detect Ki67 **(B, D)**, CD21 (follicular dendritic cell marker) **(C)**, CD3 and CD20 **(E, H)**, and CD21 and αSMA **(I)**. **(F)** T cells and B cells were visualized by immunohistochemical staining of CD3 and CD20 in serial section samples. **(G)** Shown is hematoxylin and eosin staining. Scale bars, 50 μm **(B to E, I)** and 100 μm **(F to H)**.

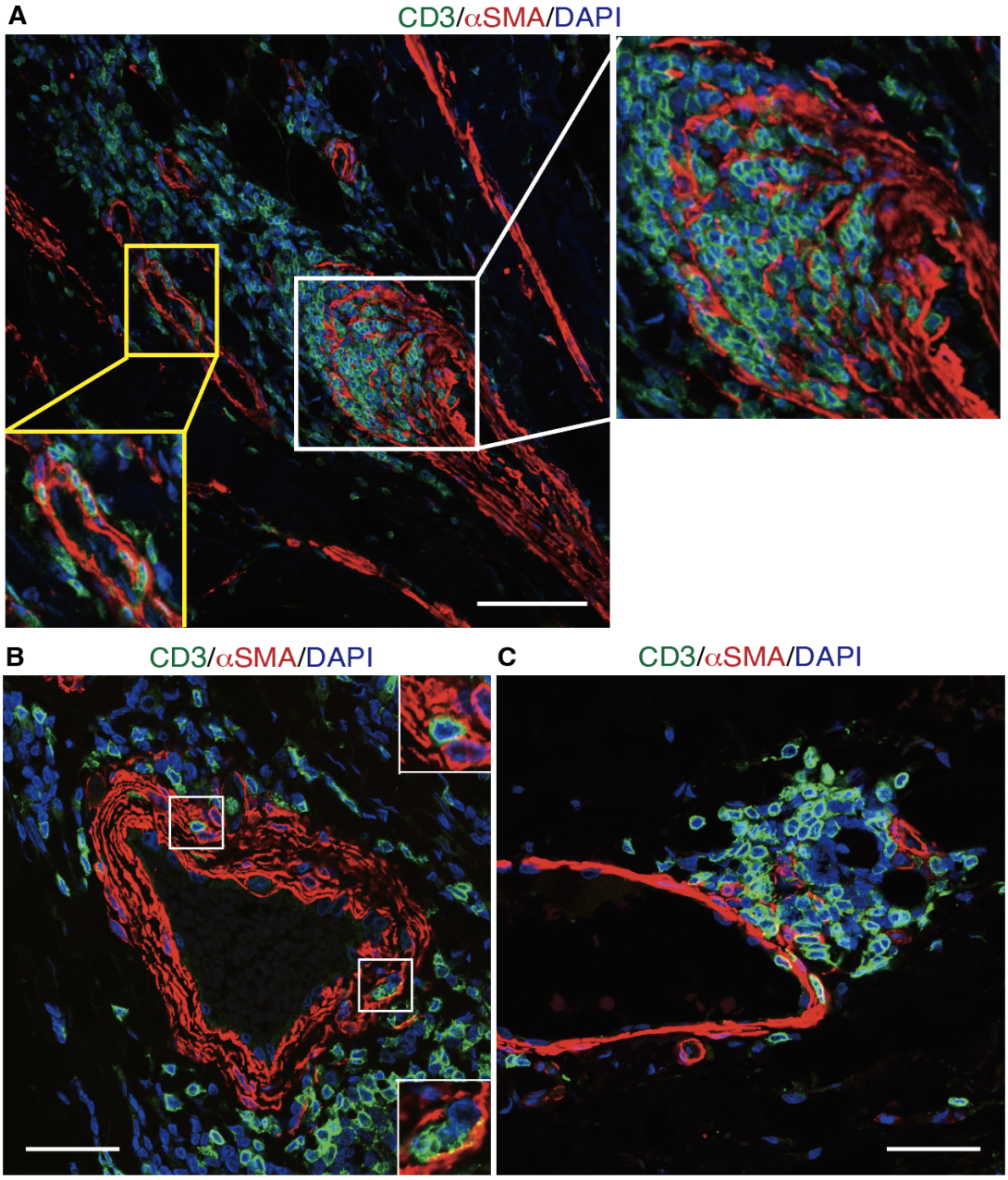

fig. S2. T cell pockets in the wall of TLS-guiding vessels. Aortic wall tissue sections from GCA aortitis were analyzed by dual-color immunofluorescence of CD3 and αSMA. **(A to C)** Shown is a TLS-guiding artery and vein **(A)**, a TLS-guiding artery **(B)** and a TLS-guiding vein **(C)**. All TLS-guiding vessels are in immediate contact with T cell clusters and contain layers of T cells embedded into their wall. Scale bars, 100 µm **(A)** and 50 µm **(B and C)**.

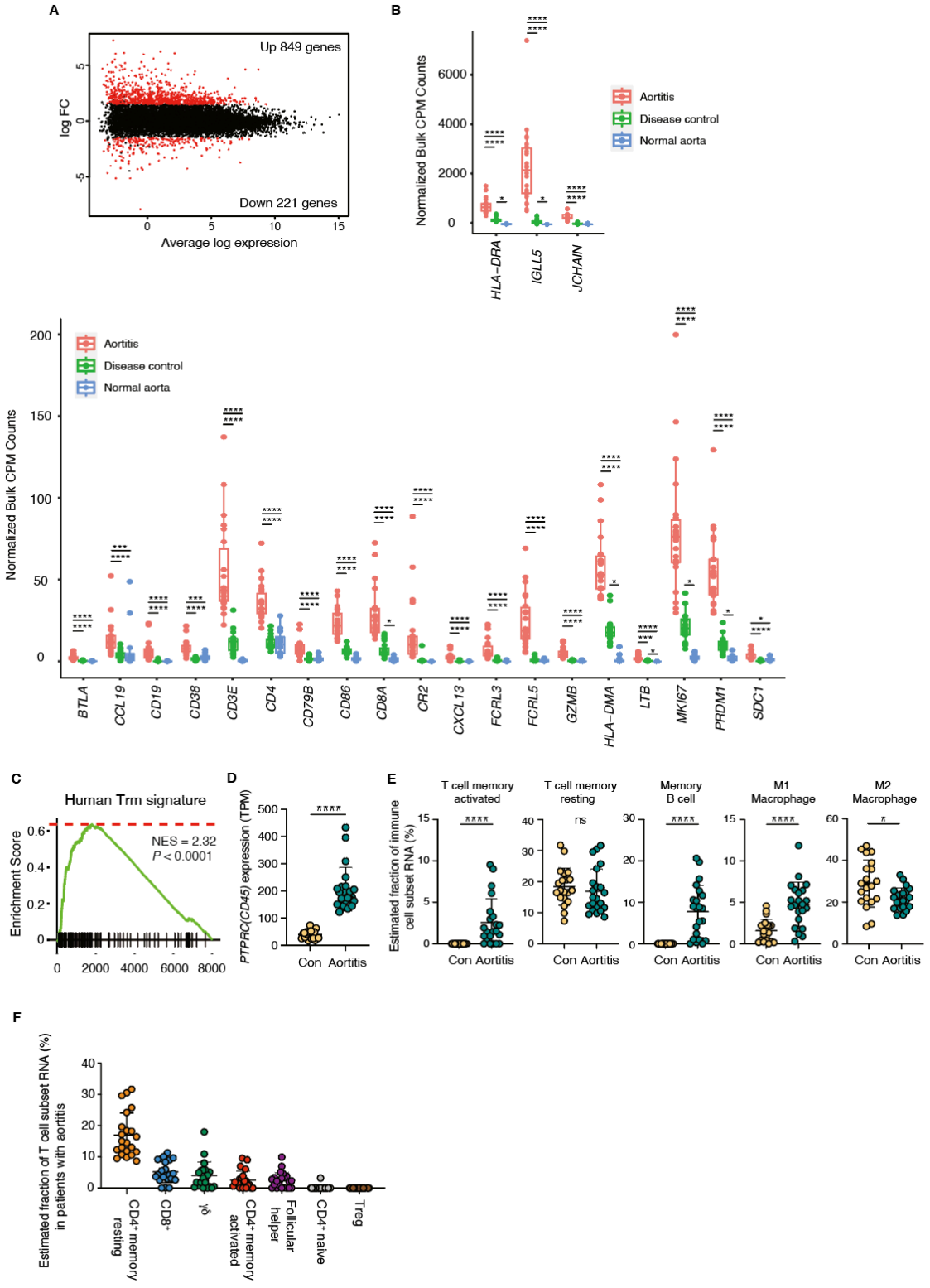
A
Up 849 genes
Down 221 genes
log FC
Average log expression
B
Normalized Bulk CPM Counts
Aortitis
Disease control
Normal aorta
HLA–DRA
IGLL5
JCHAIN
BTLA
CCL19
CD19
CD38
CD3E
CD4
CD79B
CD86
CD8A
CR2
CXCL13
FCRL3
FCRL5
GZMB
HLA–DMA
LTB
MKI67
PRDM1
SDC1
C
Human Trm signature
NES = 2.32
P < 0.0001
Enrichment Score
D
PTPRC(CD45) expression (TPM)
Con
Aortitis
E
Estimated fraction of immune cell subset RNA (%)
T cell memory activated
T cell memory resting
Memory B cell
M1 Macrophage
M2 Macrophage
ns
F
Estimated fraction of T cell subset RNA (%) in patients with aortitis
CD4+ memory resting
CD8+
γδ
CD4+ memory activated
Follicular helper
CD4+ naive
Treg

fig. S3. Transcriptomic analysis of tissues with aortitis, tissues with non-inflamed aneurysm and normal aortic wall. (A) Differentially expressed genes between aortitis and non-inflamed aortic aneurysm used as a disease control (Con). Black dots represent genes with no significant change in expression, red dots represent genes with significant change in expression. **(B)** Normalized bulk counts per million reads mapped (CPM) values of TLS-associated genes in aortitis (*n*=22), non-inflamed aortic aneurysm (*n*=20) and normal aortic tissues (*n*=12). The normal aorta data sets were extracted from GSE 141032 (*67*). Highly abundant gene transcripts (*HLA-DRA, IGLL5, JCHAIN*) are shown separately. **(C)** GSEA of human tissue resident memory T (Trm) cells in aortitis (*n*=22) and non-inflamed aortic aneurysms (*n*=20) (NES; Normalized Enrichment Score). **(D)** Comparison of transcripts per million (TPM) values of *PTPRC* (encoding CD45) in aortitis and disease control cases. **(E)** Quantitative evaluation of immune cell infiltrates as determined by CIBERSORT analysis of bulk RNA-seq data in aortitis (*n*=22) and non-inflamed aortic aneurysms (*n*=20). **(F)** Estimated proportions of T cell subpopulations in aortitis were calculated. Data are presented as mean ± SD. Data were analyzed by Kruskal-Wallis test (**B**) or Mann-Whitney *U* test (**D, E**). **P* < 0.05, ***P* < 0.01, ****P* < 0.001, *****P* < 0.0001; ns, not significant.

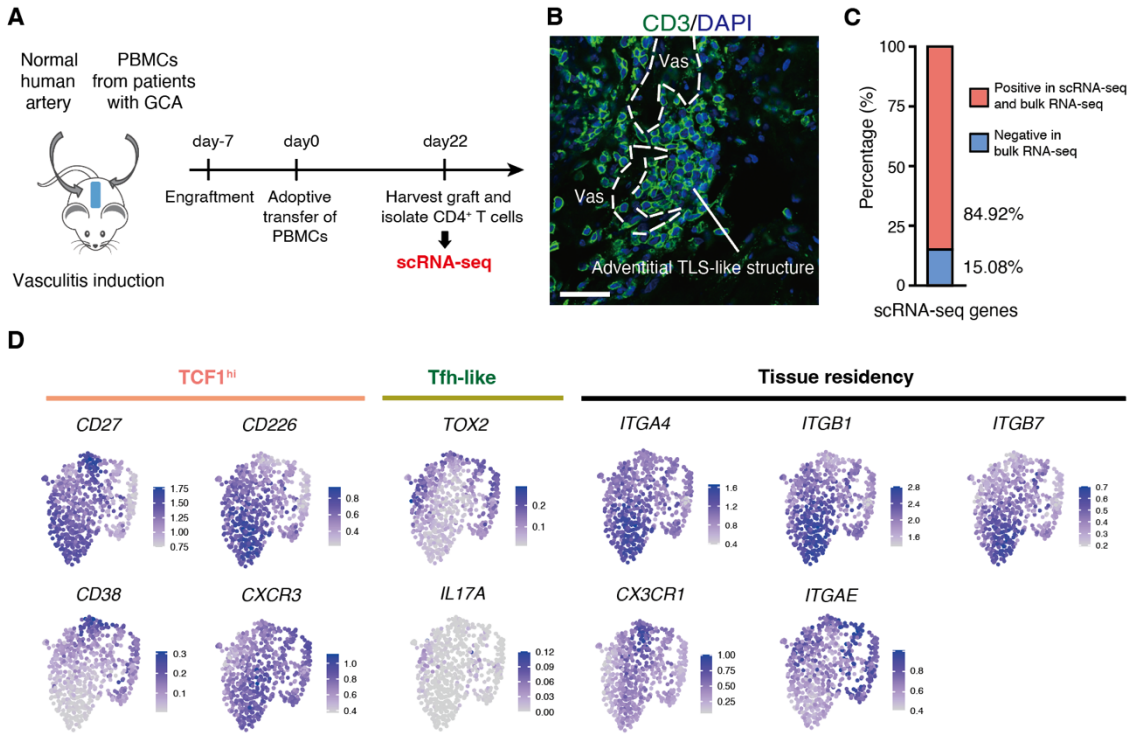

fig. S4. Transcriptomic analysis of heterogeneous tissue-residing CD4$^+$ T cells in vasculitis. (A) Experimental design of vasculitis induction in NOD scid gamma (NSG) mice engrafted with human arteries and reconstituted with patient-derived PBMCs. Explanted arteries were digested, CD4$^+$ T cells were isolated and analyzed by scRNA-seq. **(B)** T cell aggregates in the vascular tissues were identified by immunofluorescence visualizing CD3. Scale bar, 50 µm. **(C)** Proportion of the genes identified by scRNA-seq that were also identified by bulk RNA-seq of aortitis patients. **(D)** UMAP visualization of gene expression in TCF1^{hi} CD4$^+$ T cells (*CD27, CD226, CD38, CXCR3*), Tfh-like cells (*TOX2* and *IL17A*), and tissue residency related genes (*ITGAE, ITGB7, ITGB1, CX3CR1* and *ITGA4*). Data from three chimeric mice are presented.

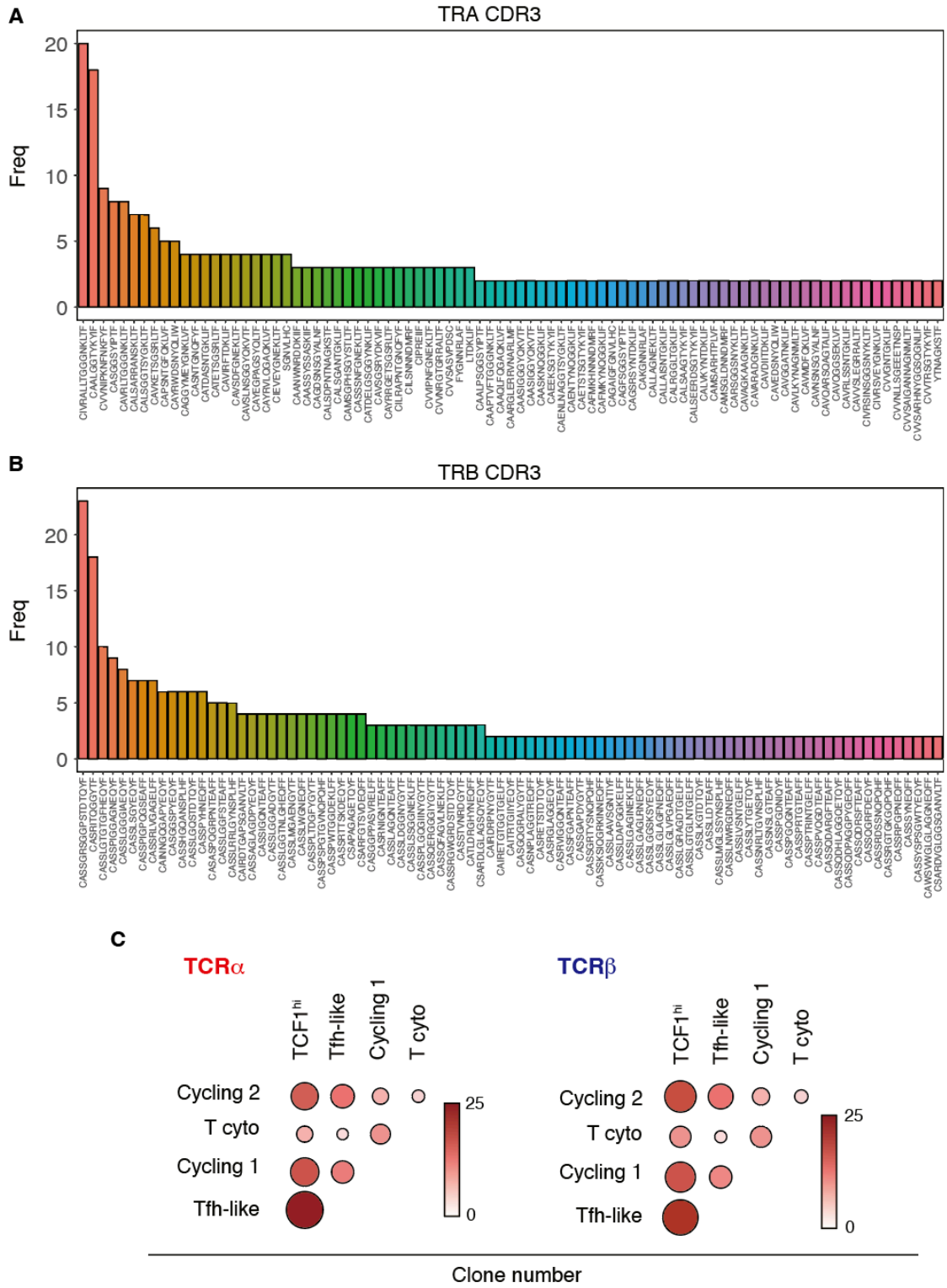
A
TRA CDR3
Freq
20
15
10
5
0
B
TRB CDR3
Freq
20
15
10
5
0
C
TCRα
TCRβ
TCF1hi
Tfh-like
Cycling 1
T cyto
Cycling 2
T cyto
Cycling 1
Tfh-like
25
0
Clone number

fig. S5. Clonal distribution of vasculogenic CD4$^+$ T cells. scTCR-seq analysis used the same cDNA starting material as used for scRNA-seq. **(A and B)** Summary data showing the size and clonal distribution of vasculogenic CD4$^+$ T cells (clonotype frequency > 1 cell). *TRA* (A) and *TRB* (B) frequency (freq) distributions are shown. **(C)** Summary chart displaying clone number overlapping among 5 distinct populations. cyto, cytotoxic.

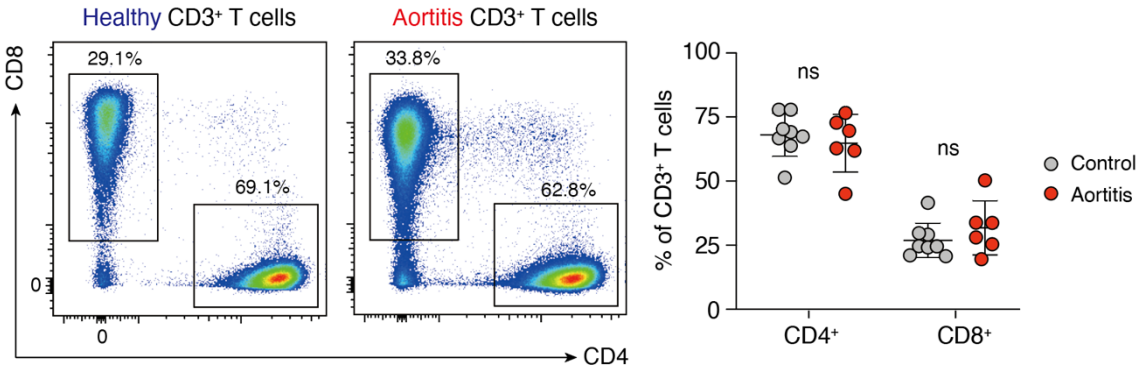

fig. S6. CD4$^+$ and CD8$^+$ T cells in aortitis patients and controls. PBMCs were collected from patients with a diagnosis of GCA aortitis (*n*=6) and age-matched healthy controls (*n*=8) and analyzed by flow cytometry. Frequencies of CD4$^+$ and CD8$^+$ T cells in aortitis patients and controls. Representative dot plots and frequencies of the T cell subsets are shown. Data are presented as mean ± SD. Data were analyzed by Mann-Whitney *U* test. ns, not significant.

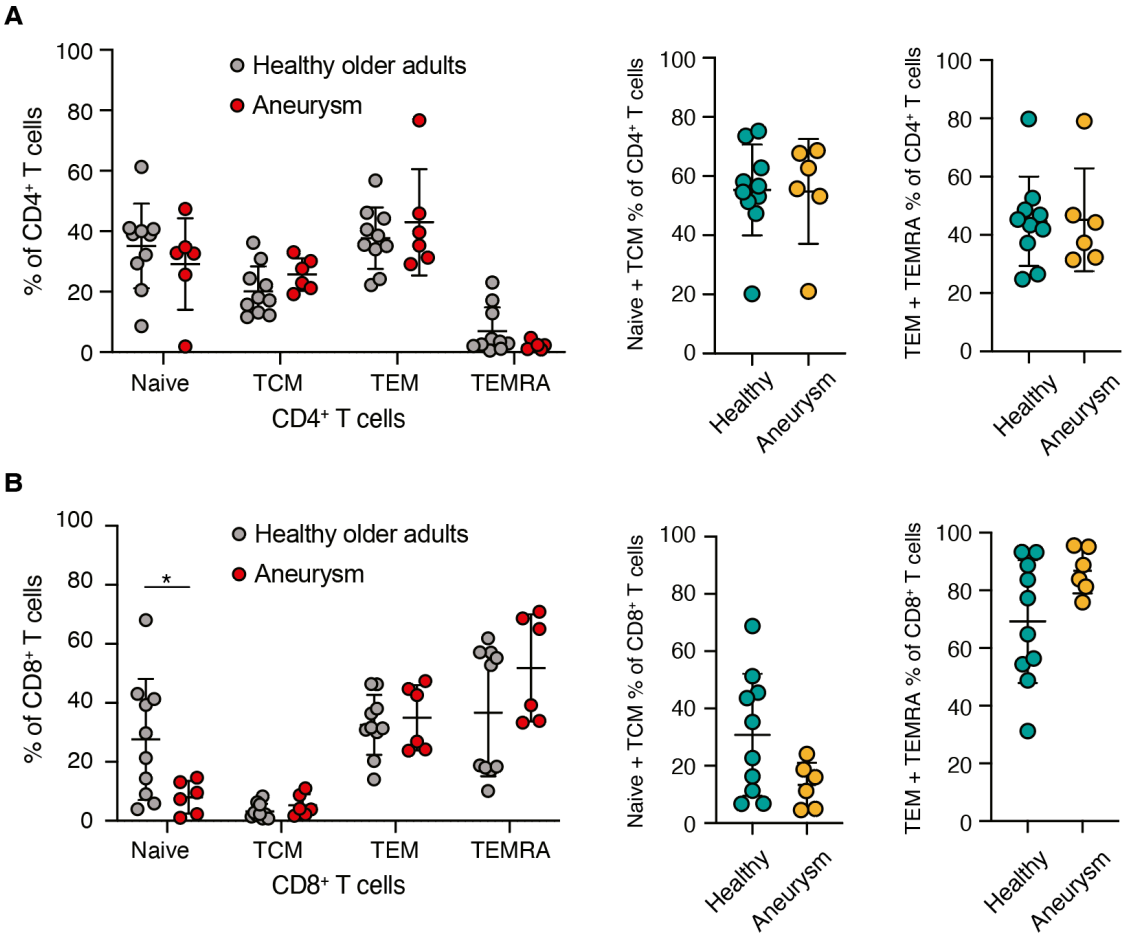

fig. S7. CD4$^+$ and CD8$^+$ T cell subsets in healthy controls and in patients with non-vasculitic aortic aneurysm. PBMCs were collected from patients with aortic aneurysm (n=6) and age-matched healthy controls (n=10) and analyzed by flow cytometry. **(A and B)** CD4$^+$ and CD8$^+$ T cells from patients with aortic aneurysm and age-matched controls were subdivided into naïve, central memory cells (TCM), effector memory cells (TEM) and effector memory cells re-expressing CD45RA (TEMRA) T cells. Frequencies of the T cell subsets and combined proportions of (naïve plus TCM) and (TEM plus TEMRA) are shown. Data are presented as mean ± SD with individual values indicated and were analyzed by unpaired two-tailed t-test (**A, B**). *$P < 0.05$.

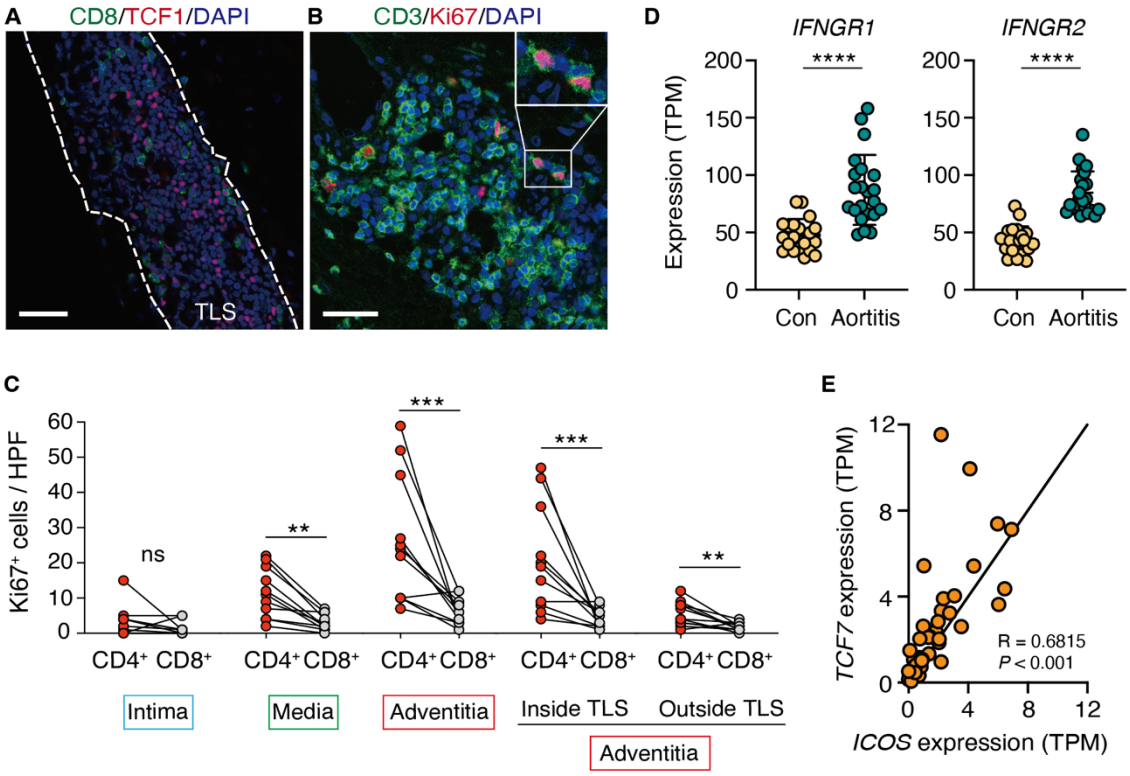

fig. S8. Characteristics of tissue-residing T cells in aortitis. T cells were analyzed by dual-color immunofluorescence and bulk RNA-seq of tissues from patients with aortitis and non-inflamed aortic aneurysm as a disease control. **(A to C)** Spatial mapping of TCF1-expressing and proliferating T cells by IF. **(A and B)** Shown is staining for CD8 and TCF1 (**A**) as well as for CD3 and Ki67 (**B**). Scale bars, 50 µm. **(C)** Geographic distribution of $CD4^+Ki67^+$ and $CD8^+Ki67^+$ T cells in the intima, the media, and the adventitia of 11 cases of GCA aortitis. HPF, high power field. **(D)** Comparison of TPM values of *IFNGR1* and *IFNGR2* in aortitis and disease controls. **(E)** Correlation between TPM values of *TCF7* and *ICOS*. Data are presented as mean ± SD. Data in (**C, D**) were analyzed by Mann-Whitney *U* test and the correlation in (**E**) was determined by Pearson's correlation analysis. $^{**}P < 0.01$, $^{****}P < 0.0001$; ns, not significant.

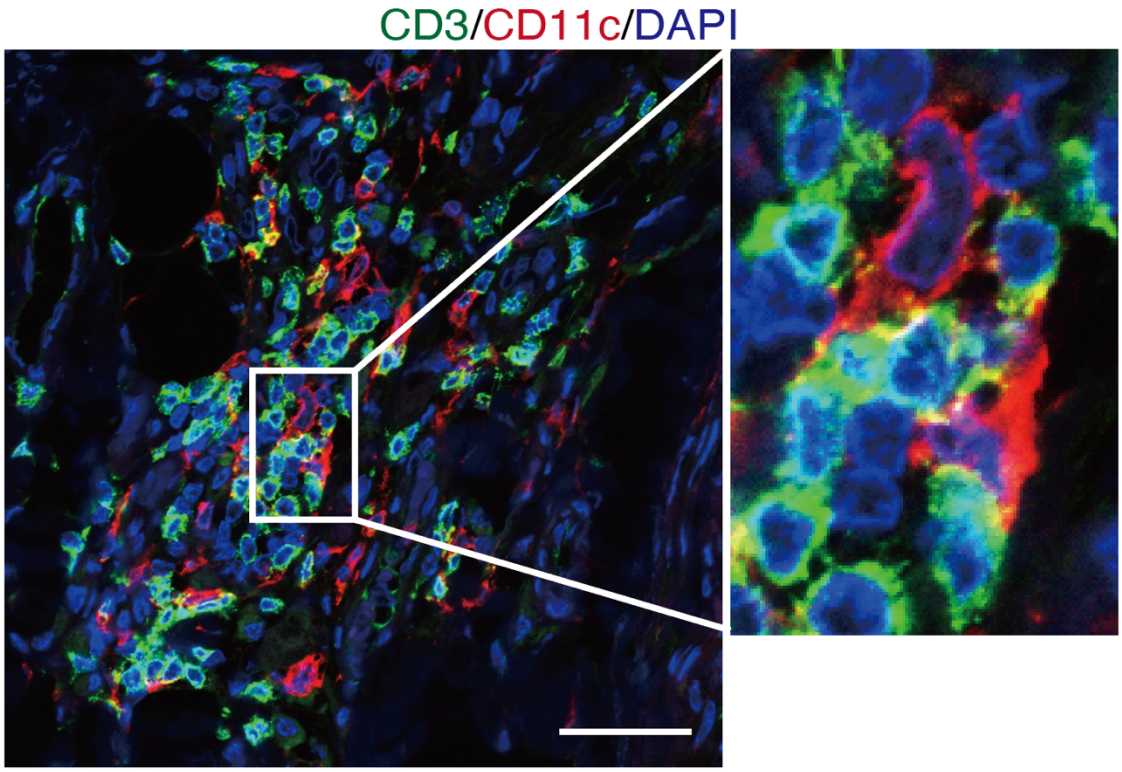

fig. S9. CD11c^{+} dendritic cells have direct contact with T cells. Immunofluorescence of CD3 and CD11c in tertiary lymphoid structures in aortic tissue from a patient with GCA aortitis. Scale bars, 50 μm.

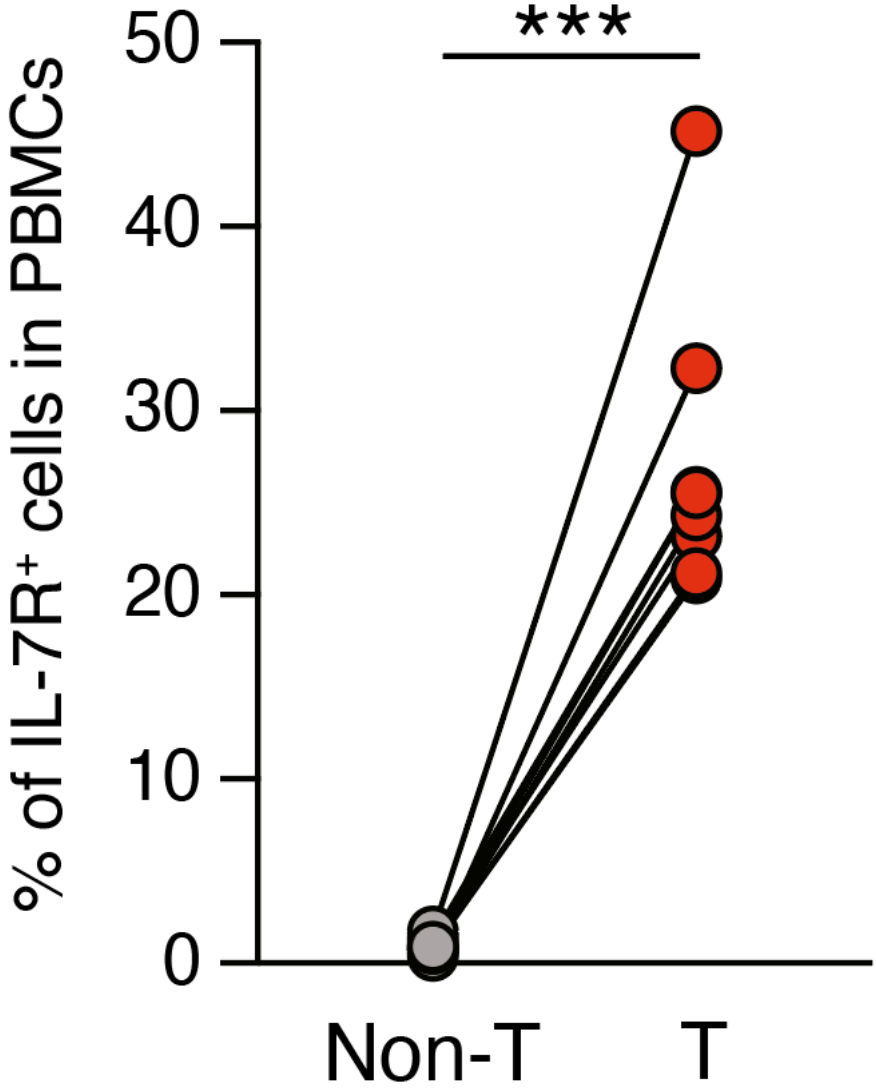

fig. S10. IL-7 receptor (IL-7R) expression is confined to T cells.

PBMCs were collected from healthy older adults and IL-7R expression was analyzed by flow cytometry (n=8). Frequencies of IL-7R-expressing T cells and non-T cells are shown. Data were analyzed by Mann-Whitney U test. ***$P < 0.001$.

Table S1. Antibody list (Immunofluorescence and Immunohistochemistry)

Antigen	Company	catalog number	Dilution
CD3	Dako	M7254	1/200
CD3	Abcam	ab5690	1/200
CD4	BIOCARE Medical	API 3209 AA	-
CD8	BIOCARE Medical	API 3219 A	-
CD11c	CST	#45581	1/200
CD20	eBioscience	#14-0202-82	1/100
CD21	Abcam	ab75985	1/400
PNAd	Biolegend	120801	1/100
aSMA	Sigma-Aldrich	C6198	1/600
vWF	Abcam	ab6994	1/200
MKi67	Abcam	ab16667	1/200
MKi67	CST	#9449	1/200
TCF1	CST	#2203S	1/200
EOMES	Thermo Fisher Scientific	50-4877-42	1/100
Podoplanin	Invitrogen	14-9381-80	1/100
Alexa Fluor 488-rabbit IgG	Thermo Fisher Scientific	A-11034	1/300
Alexa Fluor 488-mouse IgG	Thermo Fisher Scientific	A-11001	1/300
Alexa Fluor 594-Rabbit IgG	Thermo Fisher Scientific	A-21207	1/300
Alexa Fluor 594-mouse IgG	Thermo Fisher Scientific	A-11032	1/300
Alexa Fluor Plus 647-rat IgG	Thermo Fisher Scientific	A48265	1/300
Rat IgG HRP	Abcam	ab97057	1/200

Table S2. Antibody list (Flow Cytometry

Antigen	Company	catalog number	conjugated	Dilution
CD3	BioLegend	344842	BV785	1/100
CD3	BD	563546	UV395	1/200
CD4	Biolegend	344642	BV785	1/200
CD8	Biolegend	344732	BV510	1/200
TCF1	CST	14456	PE	1/100
TBX21	Biolegend	644815	BV421	1/100
CD127(IL7R)	Biolegend	351304	PE	1/100
CD45RA	BD	555488	FITC	1/50
CCR7	Biolegend	353225	PE-Cy7	1/100
CD45	Biolegend	368532	PE-Cy7	1/100

BV: Brilliant Violet, UV: Ultra Violet, PE: Phycoerythrin, FITC: Fluorescein isothiocyanate, Cy7: Cyanine7

Table S3. Primer sequence for RT-PCR

	Fw	R
ACTB	GATCATTGCTCCTCCTGAGC	CGTCATACTCCTGCTTGCTG
IFNG	ACTAGGCAGCCAACCTAAGCAAGA	CATCAGGGTCACCTGACACATTCA
GZMB	GATCATCGGGGGACATGAGG	TGACATTTATGGAGCTTCCCCA
VEGFA	GGTCGGGCCTCCGAAACCATG	GCAGCCTGGGACCACTTGGC